Applied Catalysis B: Environmental 162 (2015) 364–371

Contents lists available at ScienceDirect

Applied Catalysis B: Environmental

journal homepage: www.elsevier.com/locate/apcatb

Environmentally friendly and efficient catalysis of cyclohexane oxidation by iron meso-tetrakis(pentafluorophenyl)porphyrin immobilized on zinc oxide

Guan Huang*, Lin-Qiang Mo, Jing-Li Cai, Xuan Cao, Yan Peng, Yong-An Guo, Su-Juan Wei

College of Chemistry and Chemical Engineering, Guangxi University, Nanning 530004, China

ARTICLE INFO

Article history:
Received 23 March 2014
Received in revised form 6 June 2014
Accepted 7 July 2014
Available online 15 July 2014

Keywords:
Immobilization
Zinc oxide
Iron porphyrin
Cyclohexane
Oxidation

ABSTRACT

The use of zinc oxide-promoted catalysis of tetrakis(pentafluorophenyl)porphyrin iron chloride for cyclohexane oxidation was studied. Tetrakis(pentafluorophenyl)porphyrin iron chloride was immobilized onto zinc oxide, generating zinc oxide-supported tetrakis(pentafluorophenyl)porphyrin iron chloride, which was characterized by a variety of spectroscopic techniques and was employed to provide a stable catalyst for the oxidation of cyclohexane in the absence of any solvents or co-reductants. The small amount of tetrakis(pentafluorophenyl)porphyrin iron (1.0 μmol) in the supported catalyst could be reused 10 times for the oxidation optimized at 150 °C and 0.7 MPa. This stable catalyst provided higher turnover numbers and yields of ketone and alcohol than those obtained using the boehmite-supported tetrakis(pentafluorophenyl)porphyrin iron chloride. These results were attributed to the following factors: (1) stronger coordination of ZnO to the iron porphyrin improved its catalysis of the oxidation. (2) Improved dispersal of the iron porphyrin by ZnO enhanced the effective catalytic center. (3) Faster decomposition of peroxide into the main products.

1. Introduction

Metal porphyrin acting as a biomimetic catalyst model for the cytochrome P450 enzyme in the hydroxylation of hydrocarbons has been used for over 30 years [1,2]. Currently, at least two models of reaction conditions mimicking the hydroxylation of the substrate by P450 in vivo exist. In the first model, the reaction system contains only substrate (hydrocarbon) and catalyst. This reaction proceeds under conditions with higher than normal air pressure and above room temperatures [3–11]. These conditions are similar to those used by the Lyons catalysis system, which does not require the addition of co-reductants or stoichiometric oxidants and the use of photochemical or electrochemical techniques [12]. In the second model, the reaction system contains solvents, co-reductants and/or other additives. It proceeds at normal air pressure (i.e., 0.1 MPa) and at room temperature [13–16]. The first method is preferred in the chemical industry. However, although the second-generation metal meso-tetrakis(pentafluorophenyl)porphyrins are recognized as some of the most efficient catalysts for biomimetic oxidation reactions, they are expensive, poisonous to the environment and prone to rapid deactivation when not immobilized on a support [17]. For both the first catalytic system and the use of the supported metal polyhalogenated porphyrin catalysts, there are enormous potential industrial applications, with significant economic and environmentally friendly outcomes.

Cobalt tetraphenylporphyrin has been successfully used as a biomimetic catalyst for the aerobic oxidation of cyclohexane to cyclohexanone and cyclohexanol. It gives a catalyst turnover number (TON) of 1.1×10^4 and yields of 7–9% (KA oil), and the reaction has been industrialized in China in recent years [18]. However, there is no doubt that second-generation metal meso-tetrakis(pentafluorophenyl)porphyrins and, in particular, the corresponding supported catalysts would be more beneficial for the oxygenation of hydrocarbons [6,17,19,20]. In the present study, iron tetrakis(pentafluorophenyl)porphyrin [Fe (TPFPP)] supported on zinc oxide (ZnO) was used as a catalyst for the oxidation of cyclohexane to cyclohexanone and cyclohexanol, without the use of solvents or sacrificial co-reductants, extending the previous work by this group [10,11,19,21–23] that utilized a supported catalyst affording a catalyst TON of only $(0.7–2.5) \times 10^5$ and yields of 4.1–13.5% (KA oil). Nanoparticles of ZnO form 2-dimensional (2-D) sheet-like structures with a positive surface charge. This helps to immobilize the anionic charge on the porphyrin and promotes the catalytic oxidation of hydrocarbons [24,25]. The effect is greater

* Corresponding author. Tel.: +86 771 3237868; fax: +86 771 2851043.
E-mail addresses: huangg66@126.com, huangg6666@126.com (G. Huang).

http://dx.doi.org/10.1016/j.apcatb.2014.07.020
0926-3373/

than that for titanium and aluminum oxides [26,27], and ZnO is biosafe and biocompatible [28]. The aim of the present study was to understand the mechanism for the efficient and high yielding catalytic oxidation of cyclohexane to KA oil in the absence of any solvents, co-reductants or additives by this new ZnO-supported Fe (TPFPP) catalyst [Fe (TPFPP)/ZnO].

2. Experimental

2.1. Reagents

All reagents and solvents were of analytical grade and were obtained commercially. Fe (TPFPP) was purchased from Sigma–Aldrich Shanghai Trading Co., Ltd. (Shanghai, China). Cyclohexane was examined with gas chromatography prior to use to ensure it was free from oxidation products.

2.2. Preparation of ZnO-immobilized Fe (TPFPP)

With stirring, 70.64 g of zinc sulfate heptahydrate ($ZnSO_4{\cdot}7H_2O$) was dissolved in distilled water, and sodium hydroxide was added as the precipitation agent until pH = 8. The white zinc hydroxide precipitate that formed was filtered and washed with distilled water until no SO_4^{2-} ions could be detected. The precipitate was added to 100 ml of ethanol in a three-necked flask with stirring at high speed for 0.5 h. Subsequently, 20 mg of Fe (TPFPP), dissolved in 20 ml of absolute ethanol, was slowly added to the suspension. The mixture was heated to 60 °C with rapid stirring for 6 h. The gray suspension was filtered and washed with bulk-distilled water, and the gray cake was dried at 0.08 MPa and 160 °C for 5 h to give 20.5 g of the gray supported catalyst, Fe (TPFPP)/ZnO. The amount of immobilized metalloporphyrin in the Fe (TPFPP)/ZnO catalyst was determined using atomic emission spectroscopy with inductively coupled plasma (ICP-AES, Spectroflame model FVMØ3). The samples were digested using a traditional acid method (HNO_3 and HCl), diluted adequately and analyzed for iron. The amount of immobilized Fe (TPFPP) per gram of the supported catalyst was 0.98 mg (0.92 μmol), a value consistent with that determined using ultraviolet–visible (UV–vis) spectrophotometry [29].

2.3. Characterization of the Fe (TPFPP)/ZnO catalyst

The UV–vis spectra of the immobilized catalyst in a toluene suspension and the unsupported catalyst in a toluene solution were recorded using a PerkinElmer L-17 spectrometer.

The Fourier transform infrared (FTIR) spectra of the Fe (TPFPP)/ZnO catalyst were recorded on a PerkinElmer (model 783) IR spectrophotometer in the range 4000–400 cm^{-1} at a resolution of 2 cm^{-1} using potassium bromide (KBr) pellets.

The X-ray diffraction (XRD) patterns for the powder samples of ZnO and Fe (TPFPP)/ZnO were collected on a Rigaku D/MAX RINT 2500 X-ray diffractometer with copper (Cu) Kα radiation. Scans were performed from (2θ) 10° to 70° at a rate of 5° min^{-1}.

The particle sizes of the Fe (TPFPP) and Fe (TPFPP)/ZnO catalysts and support were measured on a Tecnai G2F20 S-TWIN transmission electron microscope with a 100 kV accelerating voltage and using a Holland Philips Ltd. Sirion 200 Field Emission Gun Scanning Electron Microscope System with a 10 or 15 kV accelerating voltage. The specific surface area (SSA) of the catalyst material samples was examined with a Build SSA-3600 porosimetry analyzer.

Thermogravimetric (TG) curves for the Fe (TPFPP)/ZnO samples were recorded using a NETZSCH STA 409 PC thermoanalyser. The measurements were conducted using 64.7 mg samples in air over a temperature range of 0–1000 °C and with a heating rate of 10 °C min^{-1}.

2.4. Use of the immobilized catalyst for cyclohexane oxidation

The catalyst material obtained by the immobilization of Fe (TPFPP) on nano-sized ZnO was used for the oxidation of cyclohexane. The oxidation was conducted in a KCF-10 500-ml autoclave reactor equipped with a magnetic stirrer and a frozen ethanol recondenser at −20 °C [22]. The mixture, which was a measured amount of the catalyst (containing 1.0×10^{-6} mol of Fe (TPFPP)) and 200 ml of cyclohexane, was stirred and heated to 150 °C. Afterward, air was continuously pumped into the reaction system and the pressure was maintained at 0.7 MPa. The set reaction conditions were optimized by experimental exploration, as described by Guo et al. [4]. The airflow was measured with a rotameter and the oxygen concentration of the tail gas was determined with a CYS-1 digital oxygen detector. Samples of the reaction mixture were identified using gas chromatography–mass spectrometry (GC–MS) and were quantified with a Shimadzu GC-16A chromatograph equipped with a 30 m × 0.32 mm × 0.5 μm FFAP capillary column and a flame ionization detector using chlorobenzene as the internal standard [23]. After the oxidation was terminated—that is, when the oxygen content in the tail gases stopped falling—the supported catalyst was recovered by simple filtration from the reaction mixture, washed with ethanol and air-dried to extract any reaction product retained in the catalyst. This supported catalyst was then used in the subsequent cyclohexane oxidation reactions.

3. Results and discussion

3.1. Characterization of the catalyst

3.1.1. UV–vis spectra of Fe (TPFPP)/ZnO

The presence of immobilized Fe (TPFPP) in the Fe (TPFPP)/ZnO material was demonstrated using UV–vis spectroscopy (Fig. 1A). The UV–vis spectra of Fe (TPFPP) and Fe (TPFPP)/ZnO shown in Fig. 1A(a) and (b), respectively, demonstrate the characteristic Soret peaks of immobilized iron porphyrin. When Fe (TPFPP) was immobilized on the ZnO support, its characteristic Soret peak was blue-shifted from 416 nm to 405 nm. The blue-shift phenomenon is opposite to the red-shifts reported elsewhere [30–35]. This means that the original saddle Fe (TPFPP) molecules were set on the surface of the ZnO crystals in a co-planar configuration. This suggests that when the original saddle (not planar) Fe (TPFPP) was immobilized on the surface of the ZnO crystal the interaction between the negative fluorine (F) atoms on the phenyl rings of the iron porphyrin and the positive zinc ion on the surface of the ZnO crystal resulted in Fe (TPFPP) becoming more planar, as previously reported [28,36]. Thus, ZnO imposed a steric pushing action on the immobilized iron porphyrin. The immobilization process increased the planarity of the porphyrin ring so that the porphyrin a_{2u} orbital (the highest occupied molecular orbital) was shifted up with respect to the e_g orbital (the lowest unoccupied molecular orbital), which then resulted in a blue-shifted Soret band. The evidence for this being the original saddle for Fe (TPFPP) was obtained in a comparison experiment: the Soret peak for TPP Fe appeared at 420 nm, whereas the Soret peak for Fe (TPFPP) appeared at 416 nm under the same conditions.

Based on the above results, the interaction between the iron porphyrin and the surface of the ZnO crystal can be described in the following two ways. The most obvious is the coordination of O atoms from ZnO into the empty orbital of the Fe ion. This interaction is accompanied by the coordination of π electrons from the porphyrin ring containing F atoms into the empty orbital of the Zn cation, as shown in Fig. 2(left), in a face-to-face/parallel orientation. Another less favorable possibility is a face-to-edge/orthogonal orientation, as shown in Fig. 2(right).

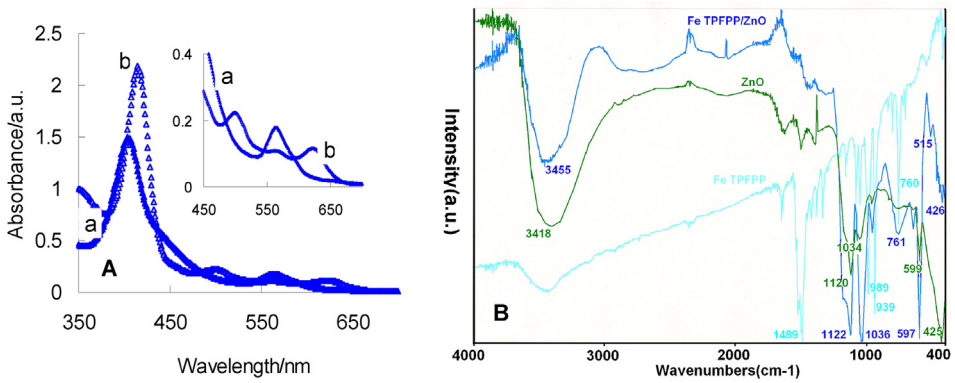

Fig. 1. (A) Ultraviolet–visible spectra at room temperature: (a) Toluene suspension of Fe (TPFPP)/ZnO [$\varepsilon = 6.76 \times 10^4$ L mol^{-1} cm^{-1}], (b) toluene solution of Fe (TPFPP) [$\varepsilon = 7.04 \times 10^4$ L mol^{-1} cm^{-1}]; (B) FTIR spectra of Fe (TPFPP)/ZnO, Fe (TPFPP) and ZnO, respectively, with an effective frequency range of 4000–400 cm^{-1}.

3.1.2. FTIR characterization of Fe (TPFPP)/ZnO

The FTIR spectra of ZnO, Fe (TPFPP) and Fe (TPFPP)/ZnO are shown in Fig. 1B. The wide band at 3418 cm^{-1} and the sharp bands at 1120 cm^{-1} and 1034 cm^{-1} are assigned to the stretching and bending vibrations of the O—H groups from the Zn(OH)$_2$ contained within the ZnO support, based on previous literature [37]. The sharp bands at 599 cm^{-1} and 425 cm^{-1} are assigned to ZnO vibrations. After Fe (TPFPP) was immobilized on ZnO, the original stretching and bending vibrations of the O—H group for the support changed little, appearing at 3455 cm^{-1}, 1122 cm^{-1} and 1036 cm^{-1}, whereas the Zn—O vibrations appeared at 597 cm^{-1} and 426 cm^{-1}. We suggest that the new peak at 515 cm^{-1} is assigned to the ZnO—Fe (TPFPP) vibration, indicating the coordination of the oxygen atom of ZnO to Fe (TPFPP). The band at approximately 1489 cm^{-1} is assigned to C=C stretching vibrations in extended aromatic domains of Fe (TPFPP) and was previously covered by the peaks of the support, that is, ZnO. A similar case reported earlier indicated that the IR bands associated with the iron porphyrin complex were not observable due to the low Fe (TPFPP) loading in this material [38]. In addition, there is another possible coordination of the O atom of ZnO via a lone electron pair to the empty anti-bonding π orbitals of the electron-deficient pentafluorophenyl rings (denoted: O→π*) and strong hydrogen bonding, such as (benzene ring)=C—F···HOZnOH···F—C=(benzene ring). All of this results in the stable immobilization of Fe (TPFPP) on zinc oxide.

3.1.3. XRD of zinc oxide immobilized Fe (TPFPP)

The characteristic diffraction peaks for the zinc oxide support are present at 31.7°, 34.4°, 36.2°, 47.5°, 56.5°, 62.8°, 66.3°, 68.0° and 69.0° and are denoted by an "a" in Fig. 3. These results are consistent with other published reports [39,40] and with that of JCPDS Card No. 36-1451. However, the support was obtained by heating zinc hydroxide at 160 °C, and so it contains a small amount of Zn(OH)$_2$, which has peaks present at 12.3°, 25.0° and elsewhere, similar to those in another report [41], labeled "b" in Fig. 3. After the small amount of Fe (TPFPP) was immobilized on the ZnO, the corresponding Fe (TPFPP)/ZnO was obtained and the original crystallinity of ZnO was changed, forming another crystal phase. The characteristic diffraction peaks appeared mainly at 12.3°, 25.0°, 32.7°, 35.0°, 36.0°, 41.0°, 51.3°, 58.5°, etc., as shown in Fig. 3. Compared with the Fe (TPFPP)/boehmite [BM] catalyst material [19], Fe (TPFPP)/ZnO

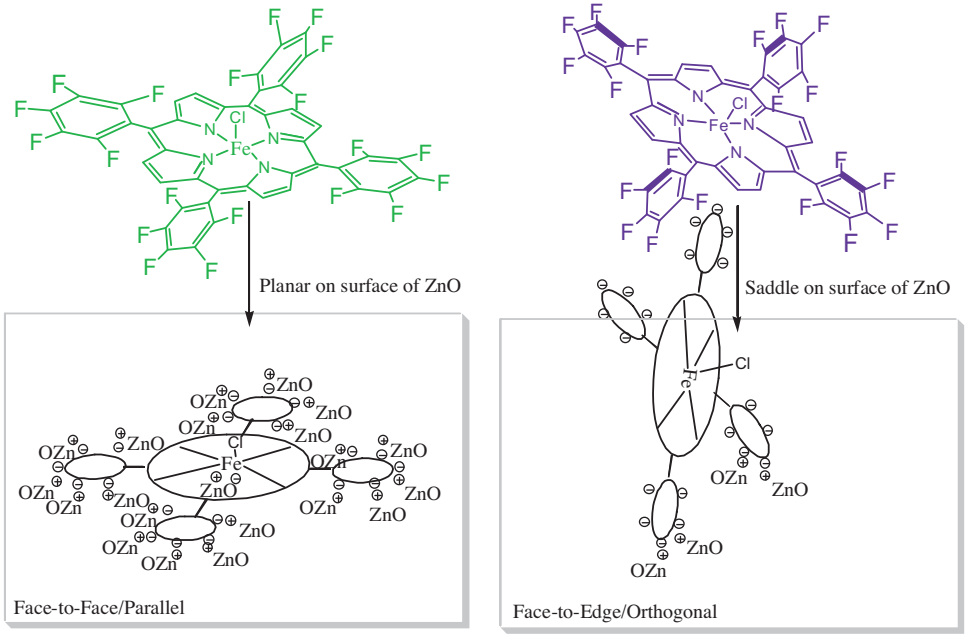

Fig. 2. Structures of the Fe (TPFPP) employed in this study and the anticipated binding geometries of the fluorine (F) derivatives on zinc oxide surfaces. This diagram shows ideal (parallel)/unfavorable (orthogonal) behavior of the supported catalyst on the zinc oxide surface. However, other binding modes are also possible. Due to the steric constraints of these systems, at least 2 of the 20 F atoms bound to the surface are needed to fix the iron porphyrin in a rigid planar structure, as depicted.

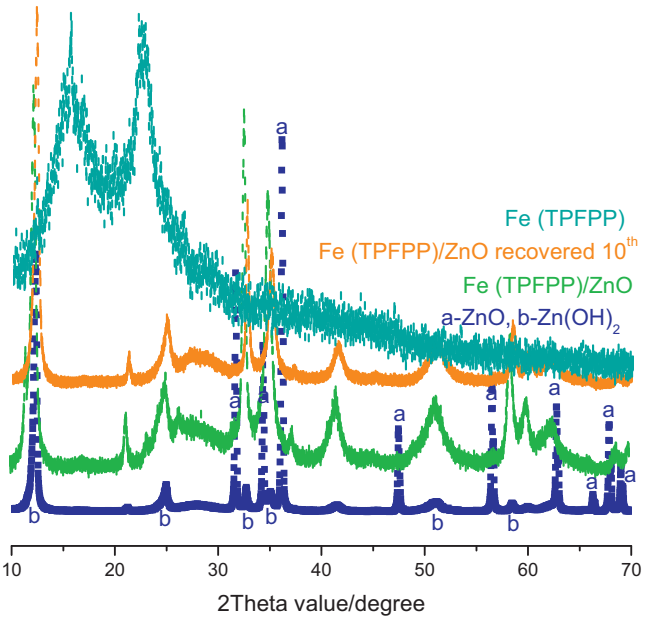

Fig. 3. X-ray diffraction (XRD) patterns of ZnO, Fe (TPFPP), and Fe (TPFPP)/ZnO after the 10th recovery.

showed better crystallinity and more crystallites, which are further demonstrated by its transmission electron microscopic (TEM) image.

3.1.4. TEM, FE-SEM and SSA characterizations of Fe (TPFPP)/ZnO

The characteristics of the surfaces of the particles were studied with TEM and field emission scanning electron microscopy (FE-SEM) images of Fe (TPFPP)/ZnO and ZnO. Fig. 4A and 4B show approximately 7 nm particles for Fe (TPFPP)/ZnO. These particles were smaller than those of ZnO and about 10 times smaller than those of Fe (TPFPP)/BM [19]. Similar to the corresponding ZnO support, Fe (TPFPP)/ZnO formed an irregular solid of layered nanoparticles and nanometer scale 2-D sheets (Fig. 4C and D). These experimental data also showed that the values for the specific surface area (SSA) of Fe (TPFPP)/ZnO and of Fe (TPFPP)/BM were 6.36 m^2/g and 0.99 m^2/g, respectively. By contrast, the "foot-print" area of the Fe (TPFPP) complex is approximately 1.77×10^{-18} m^2 because the highest diameter of metalloporphyrins is approximately 15 Å [42]. Therefore, we suggest that Fe (TPFPP) adopts a monolayer configuration anchored on the surface of ZnO. The ideal (parallel)/unfavorable (orthogonal) behavior of the Fe (TPFPP) on the zinc oxide surface shown in Fig. 2 is based on all the above data

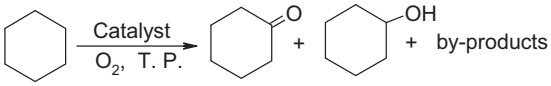

Scheme 1. Catalysis of supported iron porphyrins for oxidation of cyclohexane to cyclohexanol and cyclohexanone.

and logic. These structural characteristics of the supported catalyst should promote the catalysis of cyclohexane oxidation.

3.1.5. TG analysis of Fe (TPFPP)/ZnO

The thermostability of Fe (TPFPP)/ZnO and ZnO is critical for their use as catalysts for oxidation, and the results of their thermostability analysis are shown in Fig. 5. The weight loss for the solid catalyst and support was very modest below 220 °C and was attributed to the loss of the small quantity of $Zn(OH)_2$ contained in ZnO. This result indicates that the solid catalyst is very stable, more stable than the support ZnO under our reaction conditions. A similar stabilization of Fe (TPFPP) via immobilization was reported [43]. This process can greatly improve the reusability of the iron porphyrin for the oxidation reaction. In addition, based on the loss of Fe (TPFPP) observed as an endothermal effect centered at 370 °C [43], we suggest that the shoulder peak on the higher temperature side of the supported differential scanning calorimetric (DSC) spectrum resulted from the sublimation of Fe (TPFPP).

3.2. Oxidation of cyclohexane over Fe (TPFPP)/ZnO

The oxidation of cyclohexane over Fe (TPFPP) or zinc oxide immobilized Fe (TPFPP) produced mainly cyclohexanol and cyclohexanone. The oxidation of cyclohexane is described in Scheme 1. The support ZnO alone cannot catalyze the oxidation.

The reaction products, identified by GC–MS and chemical analysis, showed that the by-products were cyclohexyl hydroperoxide, hexanedioic acid and dicyclohexyl adipate. However, the amount of cyclohexyl hydroperoxide was very small.

For the oxidation of hydrocarbons, although, the catalytic powers of various metalloporphyrin catalysts are quite different, the catalytic mechanisms are similar [10–12,21,22,44,45]. Therefore, we propose that $^{+\bullet}$[O=Fe^{IV} TPFPP/ZnO] is the key intermediate in the catalytic oxidation of cyclohexane over the zinc oxide immobilized Fe (TPFPP) catalyst under our experimental reaction conditions, and that Fe^{III} (TPFPP)/ZnO and Fe^{II} (TPFPP)/ZnO catalyzed the decomposition of cyclohexyl hydroperoxide into the main products. A plausible mechanism for the catalytic oxidation of cyclohexane is shown in Scheme 2 and is based on our best understanding for hydrocarbon oxidation with air [46–48], the first recovered supported catalyst showing the same UV–vis spectrum

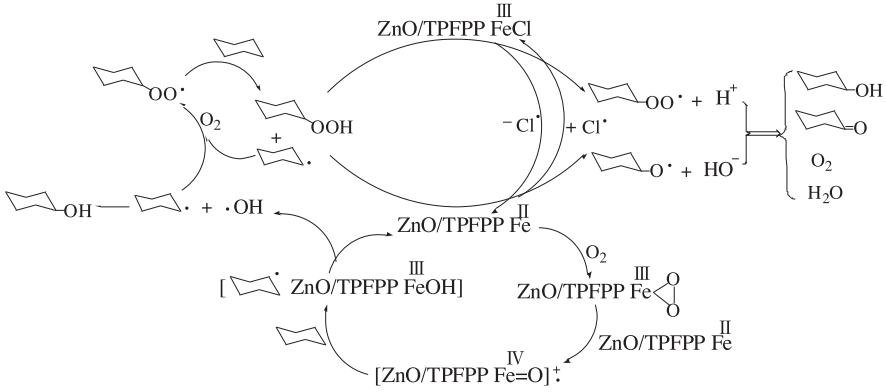

Scheme 2. A possible mechanism for the oxidation of cyclohexane over the ZnO-supported iron porphyrins.

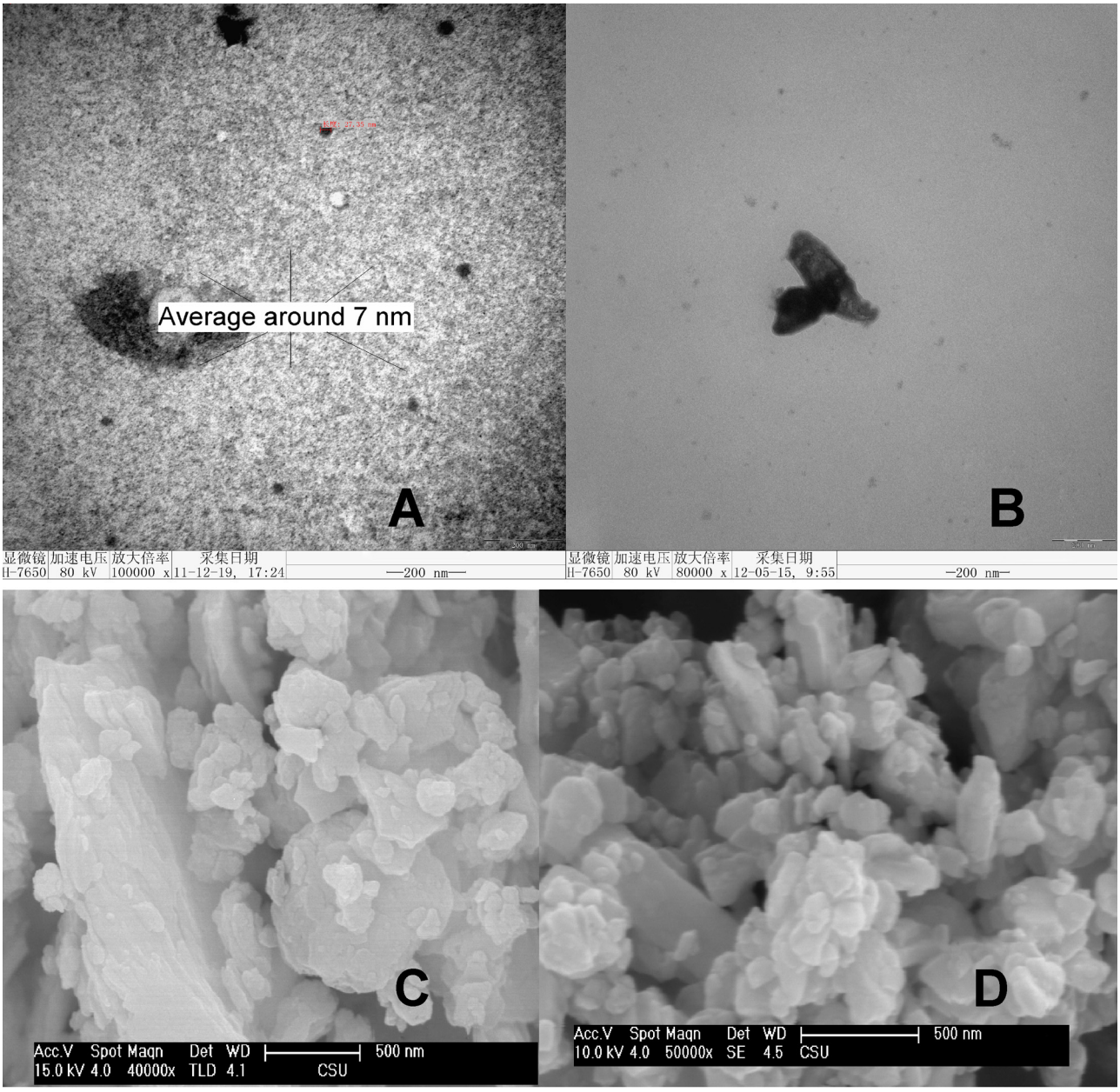

Fig. 4. Transmission electron microscopy images of Fe (TPFPP)/ZnO (A) and ZnO (B), and field emission scanning electron microscopy images of Fe (TPFPP)/ZnO (C) and ZnO (D).

as the original Fe^{III} (TPFPP)/ZnO and the very small amount of cyclohexyl hydroperoxide detected by chemical analysis.

The difference in the catalytic performance between the two catalysts, Fe (TPFPP)/ZnO and Fe^{III} (TPFPP), may originate in two ways. First, the immobilized catalyst is well protected by the coordination between the metalloporphyrin and the ZnO. Second, the coordination of the O atom of ZnO to Fe (TPFPP) promotes the catalysis of the metalloporphyrin for the hydrocarbon oxidation [22,27,46] and protects the Fe (TPFPP) from structural damage by oxidation with oxygen.

3.2.1. *Reaction temperature influences on the catalysis of Fe (TPFPP)/ZnO for oxidation of cyclohexane*

Temperature is the most important factor for oxidation. The Kp for the dissociation of molecular oxygen into atoms is 2.4×10^{-46} at 227 °C [49]. Thus, in the absence of catalysts, no free oxygen atoms exist below 227 °C. In addition, the auto-oxidation of cyclohexane yields a small amount of cyclohexanol and cyclohexanone [47], as shown in Table 1. Therefore, Fe (TPFPP) or Fe (TPFPP)/ZnO is responsible for catalyzing the oxidation of cyclohexane, and ZnO promotes the oxidation with respect to Fe-TPFPP.

Table 1
Data for catalytic activity of cyclohexane oxidation over Fe (TPFPP)/ZnO, Fe (TPFPP), ZnO and no catalyst.

Catalyst	Amount of Fe (TPFPP) (mg)	TON ($\times 10^5$)	Selectivity (%)	Yields (KA oil) (mol%)
Fe (TPFPP)/ZnO	0.5	1.5	57.1	20.4
	1.0	8.1	56.5	22.5
	1.5	5.0	60.8	22.3
Fe (TPFPP)	1.0	5.0	64.0	15.0
ZnO or no catalyst		–	87.6	3.8

Reaction conditions: 200 ml of cyclohexane, 150 °C and 0.7 MPa, reaction time = 2.5 h.

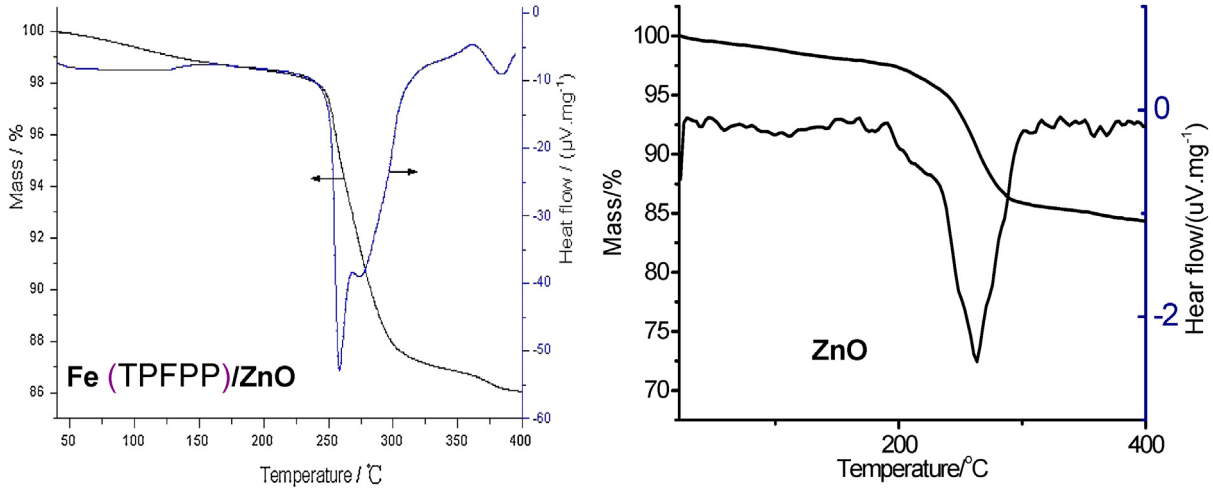

Fig. 5. Thermogravimetric and differential scanning calorimetric analysis of Fe (TPFPP)/ZnO and ZnO.

The change in the yield of the main products and catalyst TONs with the reaction times for the oxidation over Fe (TPFPP)/ZnO at various temperatures are shown in Fig. 6A. Generally, increasing the reaction temperature increased the catalyst turnover numbers and yields of KA oil. The 21.5% yields for cyclohexanone and cyclohexanol obtained in the oxidation over Fe (TPFPP)/ZnO at a reaction temperature of 155 °C were higher than those at 140 °C and 145 °C, respectively, but were close to the 17.7% yield at 160 °C and the 16.8% yield at 150 °C. Based on our research experience examining the supported metalloporphyrins, the higher the reaction temperature, the more the catalysts are damaged. Therefore, considering the aim to reuse the catalyst as many times as possible, we propose that the optimum reaction temperature is 150 °C. In addition, the higher the reaction temperature, the higher is the TON, indicating greater catalytic activity. However, too high a reaction temperature does not benefit the TON, as observed, for example, at 160 °C. We suggest that the axial coordination size of the oxygen atom in ZnO to the iron ion in Fe (TPFPP) at different temperatures is likely responsible for the changes in the TON.

In addition, increasing the temperature benefits the reaction by cleaving the Fe—Cl bonds in Fe (TPFPP)/ZnO and the O—O bonds in the peroxo complex $O_2{}^{III}$Fe (TPFPP)/ZnO promoted by the ZnO support (Scheme 2). We propose that after the oxygen atom coordination of ZnO to the central iron ion of Fe (TPFPP), the oxygen atom remains the second strongest electronegative atom and thus attracts the electron of the ZnOFe—Cl bond to itself. In addition to the opposite pull by Cl, this results in a homolytic splitting of the ZnOFe—Cl bond to produce Cl•, and the ^{II}Fe (TPFPP)/ZnO quite easily combines with O_2 to form the peroxo complex. Another aspect is that the strongest electron, drawing 20 fluorine atoms on the 4 benzene rings in Fe (TPFPP), makes the central iron ion highly positive, strongly adsorbing and activating O_2 into oxygen atoms, that is, from the peroxo complexes, $O_2{}^{III}$Fe (TPFPP)/ZnO to $^{+}$•[O=^{IV}Fe (TPFPP)/ZnO]. This process is promoted by the support ZnO, as described above.

3.2.2. *Reaction pressure influences on catalysis of Fe (TPFPP)/ZnO for cyclohexane oxidation*

The second most important factor for oxidation is air pressure. Fig. 6B shows the changes in yields (KA oil) and catalyst TONs with reaction times for cyclohexane oxidation over Fe (TPFPP)/ZnO using various reaction pressures. The oxygen concentration in the autoclave is another important factor affecting cyclohexane oxidation at a given reaction temperature. Above 0.7 MPa, the yields of KA oil fell as the reaction pressure was increased. This was because the

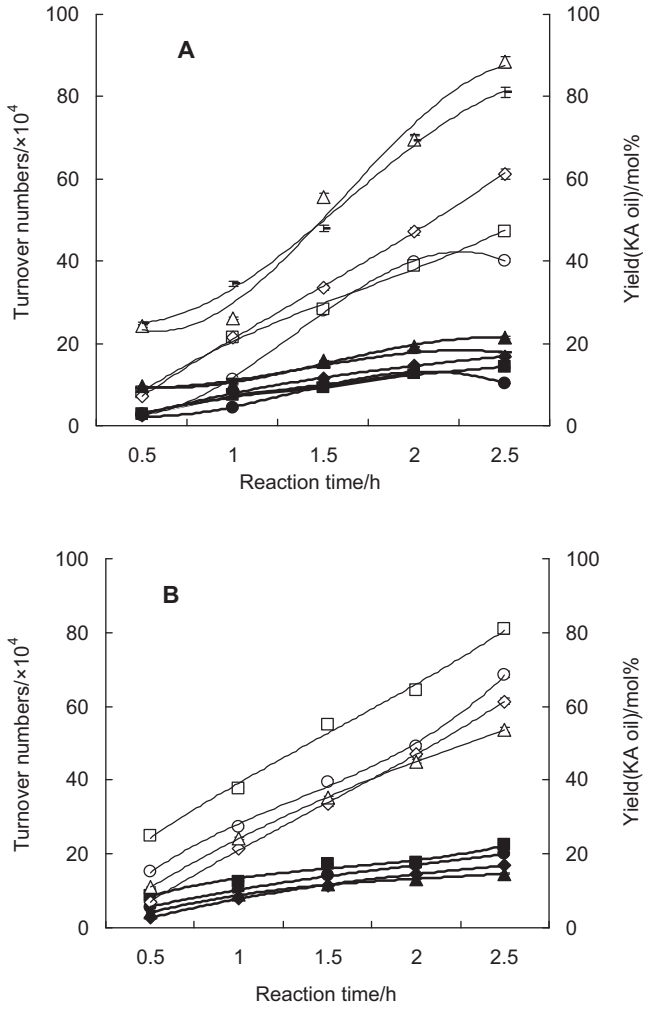

Fig. 6. (A) Changes in yields (KA oil) (solid symbols) and catalyst turnover numbers (open symbols) with reaction time for cyclohexane oxidation over Fe (TPFPP)/ZnO (containing 1.0×10^{-6} mol Fe TPFPP) at various temperatures (● and ○: 140 °C, ■ and □: 145 °C, ♦and ◊: 150 °C, ▲ and △: 155 °C and — and —: 160 °C). Reaction conditions: 200 ml of cyclohexane, 0.8 MPa, 0.040 m^3/h airflow. (B) Changes in yields (KA oil) [solid symbols] and catalyst turnover numbers [open symbols] with reaction time for cyclohexane oxidation over Fe (TPFPP)/ZnO (containing 1.0×10^{-6} mol Fe TPFPP) under different reaction pressures (● and ○: 0.6 MPa, ■ and □: 0.7 MPa, ♦and ◊: 0.8 MPa, ▲ and △: 0.9 MPa). Reaction conditions: 200 ml of cyclohexane, 150 °C, 0.040 m^3/h airflow.

Table 2
Data for catalytic activity of reused Fe (TPFPP)/ZnO and Fe (TPFPP).

Catalyst	Run	TON ($\times 10^5$)	Selectivity (%)	Yields (K + A) (mol%)	Ratio (K/A)
Fe (TPFPP)/ZnO	1	8.1	56.5	22.5	1.5
	2	5.7	62.2	16.8	1.2
	3	7.2	56.3	19.8	1.4
	4	6.9	57.6	19.2	1.3
	5	5.9	62.4	17.5	1.1
	6	6.9	55.5	18.4	1.0
	7	7.3	59.9	21.3	1.1
	8	6.5	61.1	19.0	1.2
	9	6.3	60.0	18.2	1.2
	10	6.0	62.5	17.9	1.1
	11	5.7	66.3	18.1	1.4
	Average	6.6	60.0	19.0	1.1
Fe (TPFPP)	1	5.0	64.0	15.0	1.4

Reaction conditions: 200 ml of cyclohexane, 150 °C, 0.7 MPa, Fe (TPFPP): 1.0 μmol; reaction time = 2.5 h.

Table 3
Comparison of catalytic activity of Fe (TPFPP)/ZnO(Z) with Fe (TPFPP)/BM(B).

Catalyst	TON ($\times 10^5$)	Selectivity (%)	Yields (K + A) (mol%)	Reaction conditions[a]
Z	8.10	56.5	22.5	150 °C, 0.7 MPa
B	2.66	90.3	10.9	150 °C, 0.7 MPa
Z	4.68	57.7	14.7	150 °C, 0.9 MPa
B	1.99	82.8	9.1	150 °C, 0.9 MPa
Z	4.14	63.9	14.2	145 °C, 0.8 MPa
B	2.38	87.2	9.4	145 °C, 0.8 MPa
Z	3.00	65.0	10.3	140 °C, 0.8 MPa
B	2.77	90.1	9.7	140 °C, 0.8 MPa

[a] Reaction conditions: 200 ml of cyclohexane, Fe (TPFPP): 1.0 μmol, 0.040 m^3/h airflow. Reaction time = 2.5 h.

highest TON was obtained later in the reaction, whereas the selectivity for the main products decreased with reaction time, indicating that the activity of the catalyst was reduced with the increase in reaction pressure. It is probable that too high an oxygen concentration destroyed a small fraction of the metalloporphyrins on the surface of the support. The experimental results show that 0.7 MPa is the optimum reaction pressure.

3.2.3. *The amount of Fe (TPFPP)/ZnO influences the catalysis for cyclohexane oxidation*

Table 1 presents the changes in Fe (TPFPP)/ZnO activity using different amounts of catalyst at the optimum temperature of 150 °C and air pressure of 0.7 MPa. The natural law relating activity changes to the different amounts of catalyst used was presented in our previous studies [4,5,10,11,21,22]. The most interesting results in Table 1 of the present study are that the activity of the immobilized catalyst with the optimum amount of Fe (TPFPP) (1.0 μmol) increased the TON by 62% and yield by 50% relative to those values for the corresponding unsupported Fe (TPFPP), indicating that the promotion was due to the support, which was also demonstrated by the recycling of the catalyst, as discussed below.

3.2.4. *Recycling of the Fe (TPFPP)/ZnO catalyst*

The characterization of Fe (TPFPP)/ZnO indicates that Fe (TPFPP)/ZnO was coordinated to ZnO and immobilized in a coplanar array (face-to-face) on the surface of the support. The immobilization not only highly promoted this catalyst in the oxidation of cyclohexane but also protected Fe (TPFPP) from being destroyed by O_2. This benefited the recycling of the catalyst (Table 2). Under ZnO promotion, the catalytic activity and efficiency of Fe (TPFPP) (1.0 μmol) was significantly increased, with 10-fold recycling possible. The average yield (KA oil) and TON were higher than those obtained from the same oxidation over Fe (TPFPP), and the average yield (KA oil) and conversion rate were greater than those obtained from the oxidation over Fe (TPFPP)/BM, for which reaction conditions were optimized in separate experiments [19]. Therefore, Fe (TPFPP) promoted by ZnO decomposes the cyclohexyl hydroperoxide to KA oil more quickly than that promoted by BM. The higher promotion of the catalysis of Fe (TPFPP) for the oxidation of cyclohexane by ZnO compared with that by BM is also shown in Table 3.

4. Conclusion

ZnO increased the catalytic activity of Fe (TPFPP) for cyclohexane oxidation to a greater extent than that observed using BM. First, the iron porphyrin was immobilized on the zinc oxide in a stronger coordinating model that involved the orbital structure and special electronegativity of the Zn ion. Second, the immobilization of Fe (TPFPP) on ZnO formed more and smaller nanoparticles of catalyst than those formed using BM as determined with TEM (particle diameter ratio of approximately 1/10), resulting in an increase in the number of effective active centers. Third, ZnO more rapidly promoted the catalysis of Fe (TPFPP) for cyclohexane oxidation; that is, Fe (TPFPP)/ZnO promoted the rapid decomposition of cyclohexyl hydroperoxide into the main products.

Acknowledgements

This research was supported by the National Natural Science Foundation of China (Nos.: 51063001 and 51363001), the Guangxi Scientific and Technological Project (12118008-12-3), the Guangxi Natural Science Foundation (2012GXNSFAA053016) and the Experimental Innovation Project Foundation of Guangxi University, PR China (20120322).

References

[1] J.T. Groves, R. Quinn, Inorg. Chem. 23 (1984) 3844–3846.
[2] F. Wypych, A. Bail, M. Halma, S. Nakagaki, J. Catal. 234 (2005) 431–437.
[3] C.C. Guo, M.F. Chu, Q. Liu, Y. Liu, D.C. Guo, X.Q. Liu, Appl. Catal. A: Gen. 246 (2003) 303–309.

[4] C.C. Guo, G. Huang, X.B. Zhang, D.C. Guo, Appl. Catal. A: Gen. 247 (2003) 261–267.
[5] C.C. Guo, X.Q. Liu, Y. Liu, Q. Liu, M.F. Chu, X.B. Zhang, J. Mol. Catal. A: Chem. 192 (2003) 289–294.
[6] J. Haber, L. Matachowski, K. Pamin, J. Połtowicz, Catal. Today 91–92 (2004) 195–198.
[7] J. Połtowicz, K. Pamin, L. Matachowski, E.M. Serwicka, R. Mokaya, Y. Xia, Z. Olejniczak, Catal. Today 114 (2006) 287–292.
[8] R.X. Wang, B.J. Gao, W.Z. Jiao, Appl. Surf. Sci. 255 (2009) 4109–4113.
[9] R.X. Wang, W.Z. Jiao, B.J. Gao, Appl. Surf. Sci. 255 (2009) 7766–7772.
[10] G. Huang, S.Y. Liu, Y.A. Guo, A.P. Wang, J. Luo, C.C. Cai, Appl. Catal. A: Gen. 358 (2009) 173–179.
[11] G. Huang, T.M. Li, S.Y. Liu, M.G. Fan, Y.X. Jiang, Y.A. Guo, Appl. Catal. A: Gen. 371 (2009) 161–165.
[12] J.E. Lyons, P.E. Ellis Jr., H.K. Myers Jr., J. Catal. 155 (1995) 59–73.
[13] P. Zucca, C. Vinci, A. Rescigno, E. Dumitriu, E. Sanjust, J. Mol. Catal. A: Chem. 321 (2010) 27–33.
[14] J. Połtowicz, E. Bielanska, M. Zimowska, E.M. Serwicka, R. Mokaya, Y. Xia, Top. Catal. 52 (2009) 1098–1104.
[15] M. Moghadam, V. Mirkhani, S. Tangestaninejad, I. Mohammdpoor-Baltork, H. Kargar, J. Mol. Catal. A: Chem. 288 (2008) 116–124.
[16] B. Fu, P. Zhao, H.C. Yu, J.W. Huang, J. Liu, L.N. Ji, Catal. Lett. 127 (2009) 411–418.
[17] Y. Iamamoto, M.D. Assis, K.J. Ciuffi, H.C. Sacco, L. Iwamoto, A.J.B. Melo, O.R. Nascimento, C.M.C. Prado, J. Mol. Catal. A: Chem. 109 (1996) 189–200.
[18] Y.B. She, L.Z. Wang, X.F. Song, Y.H. Zhang, Y.X. Chen, Fine Chem. 22 (2005) 401–408.
[19] G. Huang, Z.-C. Luo, Y.-D. Hu, Y.-A. Guo, Y.-X. Jiang, S.-J. Wei, Chem. Eng. J. 195–196 (2012) 165–172.
[20] J.T. Groves, M. Bonchio, T. Carofiglio, K. Shalyaev, J. Am. Chem. Soc. 118 (1996) 8961–8962.
[21] G. Huang, Z.C. Luo, F. Xiang, X. Cao, Y.A. Guo, Y.X. Jiang, J. Mol. Catal. A: Chem. 340 (2011) 60–64.
[22] G. Huang, F. Xiang, T.M. Li, Y.X. Jiang, Y.A. Guo, Catal. Commun. 12 (2011) 886–889.
[23] G. Huang, Y.A. Guo, H. Zhou, S.K. Zhao, S.Y. Liu, A.P. Wang, J.F. Wei, J. Mol. Catal. A: Chem. 273 (2007) 144–148.
[24] Y. Hong, C.G. Tian, B.J. Jiang, A.P. Wu, Q. Zhang, G.H. Tian, H.G. Fu, J. Mater. Chem. A 1 (2013) 5700–5708.
[25] G.S. Machado, F. Wypych, S. Nakagaki, J. Colloid Interface Sci. 377 (2012) 379–386.
[26] L.B. Zhang, A.J. Patil, L. Li, A. Schierhorn, S. Mann, U. Gosele, M. Knez, Angew. Chem. 121 (2009) 5082–5085.
[27] W.J. Zhang, P.P. Jiang, P.B. Zhang, P. Liu, Catal. Lett. 142 (2012) 1512–1519.
[28] F. Werner, J.F. Gnichwitz, R. Marczak, E. Palomares, W. Peukert, A. Hirsch, D.M. Guldi, J. Phys. Chem. B 114 (2010) 14671–14678.
[29] P.R. Cooke, J.R.L. Smith, J. Chem. Soc. Perkin Trans. 1 (1994) 1913–1923.
[30] G.S. Machado, K.A.D.F. Castro, F. Wypych, S. Nakagaki, J. Mol. Catal. A: Chem. 283 (2008) 99–107.
[31] M. Halma, A. Bail, F. Wypych, S. Nakagaki, J. Mol. Catal. A: Chem. 243 (2006) 44–51.
[32] S. Nakagaki, K.A.D.F. Castro, G.S. Machado, M. Halma, S.M. Drechsel, F. Wypych, J. Braz. Chem. Soc. 17 (2006) 1672–1678.
[33] H. Kameyama, H. Suzuki, A. Amano, Chem. Lett. 7 (1988) 1117–1120.
[34] M. Gouterman, J. Mol. Spectrosc. 6 (1961) 138–163.
[35] G.S. Machado, G.G.C. Arízaga, F. Wypych, S. Nakagaki, J. Catal. 274 (2010) 130–141.
[36] J. Rochford, D. Chu, A. Hagfeldt, E. Galoppini, J. Am. Chem. Soc. 129 (2007) 4655–4665.
[37] V. Ischenko, S. Polar, D. Grote, V. Stavarache, K. Fink, M. Driess, Adv. Funct. Mater. 15 (2005) 1945–1954.
[38] M.E. Lipińska, S.L.H. Rebelo, C. Freire, J. Mater. Sci. (2014), http://dx.doi.org/10.1007/s10853-013-7830-7.
[39] Y. Liu, J.-E. Zhou, A. Larbot, M. Persin, J. Mater. Process. Technol. 189 (2007) 379–383.
[40] N. Samaele, P. Amornpitoksuk, S. Suwanboon, Powder Technol. 203 (2010) 243–247.
[41] I. Grobelsek, B. Rabung, M. Quilitz, M. Veith, J. Nanopart. Res. 13 (2011) 5103–5119.
[42] S. Nakagaki, F. Wypych, J. Colloid Interface Sci. 315 (2007) 142–157.
[43] N. Bizaia, E.H. de Faria, G.P. Ricci, P.S. Calefi, E.J. Nassar, K.A.D.F. Castro, S. Nakagaki, K.J. Ciuffi, R. Trujillano, M.A. Vicente, A. Gil, S.A. Korili, ACS Appl. Mater. Interface 1 (2009) 2667–2678.
[44] N.A. Stephenson, A.T. Bell, J. Am. Chem. Soc. 127 (2005) 8635–8643.
[45] W. Nam, S.W. Jin, M.H. Lim, J.Y. Ryu, C. Kim, Inorg. Chem. 41 (2002) 3647–3652.
[46] R.A. Sheldon, J.K. Kochi, Metal-catalyzed Oxidations of Organic Compounds, Academic Press, New York, USA, 1981, pp. 109.
[47] C.A. Tolman, J.D. Druliner, P.J. Krusic, M.J. Nappa, W.C. Seidel, I.D. Williams, S.D. Ittel, J. Mol. Catal. 48 (1988) 129–148.
[48] E. McCandlish, A.R. Miksztal, M. Nappa, A.Q. Sprenger, J.S. Valentine, J.D. Stong, T.G. Spiro, J. Am. Chem. Soc. 102 (1980) 4268–4271.
[49] H. Johnston, M. Walker, J. Am. Chem. Soc. 55 (1933) 187–193.